Thermal and radiation design considerations for CubeSats in low lunar orbit

Bruno Mattos[1], Lucas Anderson[2], Randy Jost[1], Charles Swenson[1], Denis Vieira[3], and Renan Menezes[3]

[1]Center for Space Engineering
Utah State University
4130 Old Main Hill, Logan, Utah 84321
a02344836@usu.edu

[2]Orion Space Solutions
Century Place, #1000, Louisville, CO 80027

[3]Centro Espacial ITA
Instituto Tecnlógico de Aeronáutica
Praça Marechal Eduardo Gomes, 50, São José dos Campos/SP, 12228-900, Brazil

ABSTRACT

NASA's Artemis program is turning the attention back to the Moon. As an example of Artemis I, CubeSats can now be inserted into lunar orbits by ridesharing. Designers must become familiarized with the additional technical challenges of operating far away from the usual low Earth orbit (LEO) condition, especially regarding the lunar radiation and thermal environments. This paper analyzes the thermal environment loads for a spacecraft operating in a low lunar orbit (LLO) at 100km altitude with a fixed nadir-pointing orientation. A simplified thermal model is presented to assess the impact of the surfaces' thermal-optical properties and internal thermal resistances on the maximum dissipation power for 6U and 12U CubeSats at different orbital Beta-Sun angles. The occurrences of Solar eclipses in the next decade are reviewed, as well as the impact on the required heating energy to keep the CubeSats in the safe temperature range during the longest eclipse of the series. The radiation analysis focuses on the total ionization dose received by the spacecraft in LLO compared to LEO. The impact of a full-body radiation shielding approach on the chassis mass is also assessed for different wall thicknesses.

INTRODUCTION

Clusters of SmallSats are leaving Earth towards a more challenging space environment: the Moon. In late 2022, as part of NASA's CubeSat Launch Initiative (CSLI), the Artemis I mission placed 10 CubeSats on a trajectory to the Moon alongside its primary payload, the Orion spacecraft. On board the Space Launch System (SLS) rocket, the CubeSats are deployed from the Orion Stage Adapter (OSA), which can support up to 17 berths for 6U and 12U CubeSats[1]. If the Artemis program succeeds in following its schedule, four additional SLS launches are expected to happen by 2030, which can provide rideshare opportunities for up to 68 additional lunar CubeSats. Moreover, several private launches are also planned under the Commercial Lunar Payload Services (CLPS) program, which can lead to additional rideshare opportunities.

The experience from the first CubeSat on the Moon, called CAPSTONE (launched in mid-2022), and later from the series of CubeSats deployed by Artemis I shows that even the first days of operations in deep space can be extremely problematic. After a trajectory correction maneuver, CAPSTONE experienced an issue in one of its eight thrusters that caused the spacecraft to tumble beyond its attitude control capacity. After days of attempts, CAPSTONE was successfully recovered and continued its mission[2]. More than half of the 10 CubeSats launched on the Artemis I mission suffered a wide range of problems after deployment that, at a minimum, jeopardized their missions.

Beyond the Launch and Early Orbit Phase challenges, the lunar spacecraft needs to survive the Moon's harsh orbital environment for its design mission duration. Compared to low Earth orbit (LEO) missions, the lunar thermal and radiation environment stand out as the main threats to a CubeSat, which need to be adequately addressed in the design to increase survivability. This study offers a general analysis of the thermal and radiation environment for low lunar orbits (LLO). The objective is to provide data and insights useful on the conceptual design phase of future lunar CubeSats missions.

The Lunar Thermal Environment section covers the following:

- Environmental thermal loads experienced at each satellite face during one orbit at different Beta-Sun angles;
- Solar eclipses occurrences and duration in the next 10 years;

- Simplified thermal model for a CubeSat to estimate the maximum orbital dissipation power for different thermal-optical properties values;
- Maximum dissipation power for a 6U CubeSat at 100km altitude orbit as a function of thermal-optical properties;
- Maximum dissipation power for a 12U CubeSat at 100km altitude orbit as a function of thermal-optical properties;
- Surface coating selection and maximum dissipation power as a function of internal thermal resistance;
- Heating energy required to keep internal temperature over -20°C during the long-lasting eclipse.

The Lunar Radiation Environment section covers the following:

- Total Ionization Dose (TID) for a 1-year mission in LLO considering solar proton fluence in comparison to LEO considering solar proton fluence and trapped radiation;
- TID from Solar Particle Events (SPE);
- Chassis mass for full-body shielding.

LUNAR THERMAL ENVIRONMENT

Different from Earth, which has an average black body temperature of 255K with small variation across the globe and independent of the Sun illumination conditions[3], the Moon has an extreme surface temperature gradient that peaks at around 390K over the subsolar point and fades to about 90K on the dark side, see Figure 1. Since the IR radiation flux is directly proportional to the fourth power of the temperature, the spacecraft flying over the Moon's subsolar region (red on Figure 1) is subjected to more than four times the IR flux received by a spacecraft in LEO. On the Moon's night side, however, the IR flux drops significantly to less than 2% of the level experienced in LEO.

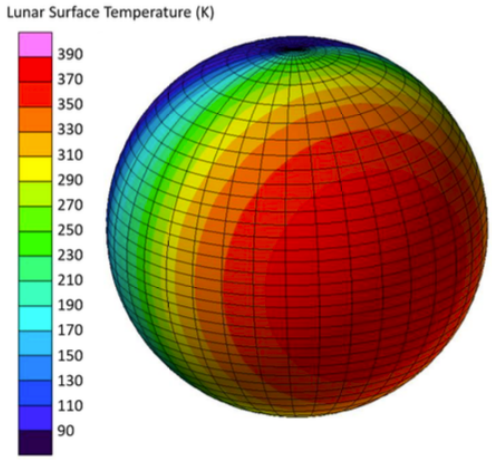

Figure 1: Lunar Surface Temperature[4]

Based on the surface temperature gradient model, the Moon's IR flux Q_{IR} can be computed by Equation 1, which uses the Sub-solar Coordinate System[4].

If $Lat_{ss} \geq 0°$

$$Q_{IR} = sin(Lat_{ss})[(1-a)S_0\sigma\epsilon T_{Dark}^4] + \sigma\epsilon T_{Dark}^4 \quad (1)$$

Otherwise,

$$Q_{IR} = \sigma\epsilon T_{Dark}^4$$

where

Lat_{ss}: degrees latitude from subsolar point (Subsolar Coordinate System)

a: Lunar surface albedo

ϵ: lunar surface emissivity

σ: Stefan-Boltzmann constant

S_0: Solar flux

T_{Dark}: unilluminated lunar surface temperature

An important aspect being considered during the thermal analysis of an LLO mission is the orbital inclination since it affects the Beta-Sun angle range and drift rate. Figure 2 presents the Beta-Sun angle drifting over a 1-year mission for 100km altitude orbits at 30°, 60°, and 90° inclination. The plot highlights two critical regions for thermal analysis. The red region corresponds to low Beta-Sun angles, where the spacecraft flies, on every orbit, over the sub-solar region and receives an intense IR flux, mainly on its nadir face. The yellow region corresponds to absolute high Beta-Sun angles, only reached by high inclination orbits. When the spacecraft is in the yellow region, it receives uninterrupted solar flux on its side; but mild IR flux since it is over the terminator region. For a polar orbit at 100km altitude, the Beta-Sun angle goes from 0° to

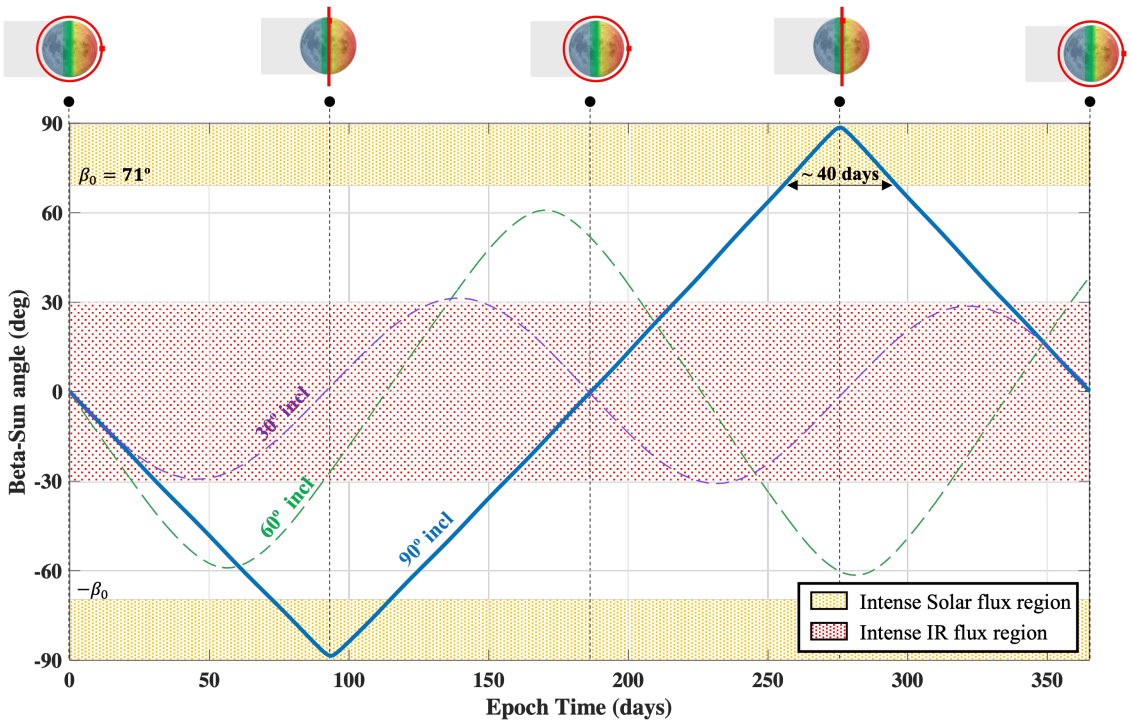

Figure 2: Beta-Sun Angle Over Time for Low Lunar Orbits at 100km Altitude

90° every three months and stays on the yellow region for about 40 days.

The IR flux received by any spacecraft face can be computed by integrating the contribution of every patch of the Moon's surface. Consider that the Moon's surface is discretized into N small plane patches as shown by Figure 3.

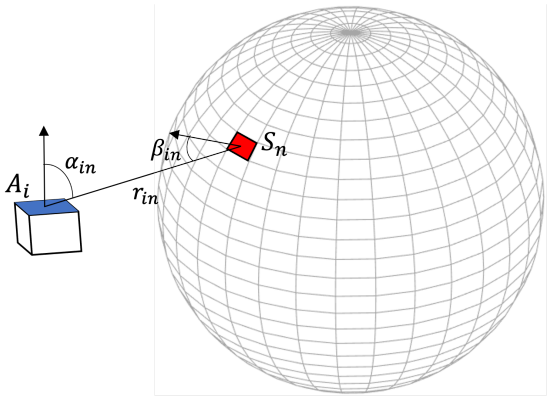

Figure 3: View Factor Geometry Definition

The total IR flux received by the face i, $P_{IR,i}$, can be computed using Equation 2.

$$P_{IR,i} = \sum_{n=0}^{N-1} Q_{IR,n} \epsilon_i A_i F_{n \to i} S_n \tag{2}$$

where

$Q_{IR,n}$: surface IR flux computed for the patch n using Eq. 1

ϵ_i: face i emissivity

A_i: spacecraft face i area

$F_{n \to i}$: view factor from surface patch n to spacecraft face i

S_n: area of lunar surface patch n

The view factor from any surface patch n to the spacecraft face i can be computed using Equation 3.

$$\begin{cases} F_{n \to i} = \frac{cos(\beta_{in}) cos(\alpha_{in}) dS_n}{\pi r_{in}^2}, & \text{if } \alpha_{in} < 90°, \beta_{in} > 90° \\ F_{n \to i} = 0, & \text{otherwise} \end{cases} \tag{3}$$

where the angles β_{in} and α_{in}, and the distance r_{in} are as defined on Figure 3.

Figures 4 and 5 present the IR radiation flux computed for one orbit period at Beta-Sun angle 0° and 90°, respectively. The spacecraft is assumed to have a fixed nadir-pointing orientation throughout the orbit.

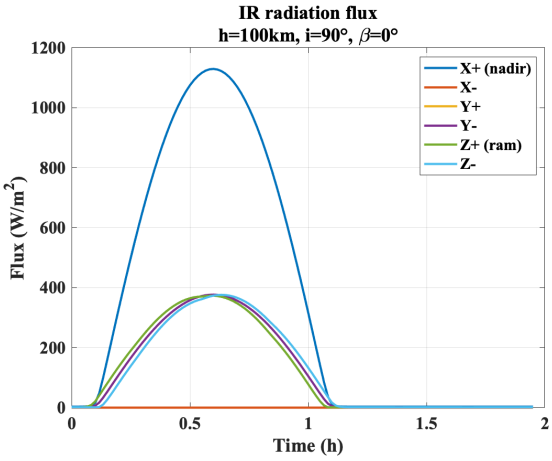

Figure 4: IR Radiation Flux on Faces during Orbital Period (0° Beta-Sun Angle)

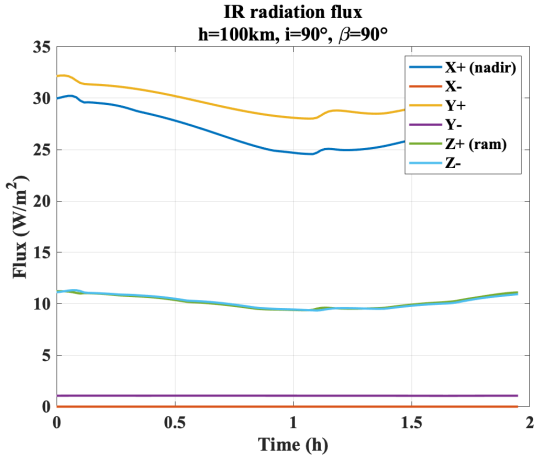

Figure 5: IR Radiation Flux on Faces during Orbital Period (90° Beta-Sun Angle)

Assuming a solar constant of $1361 W/m^2$ and a surface albedo of 0.07, the total solar radiation flux (direct + reflected) received by each face is presented in Figures 6 and 7 for Beta-Sun angle 0° and 90°, respectively.

Table 1: Orbital Average Flux for Polar LLO (h=100km)

Face	$\beta = 0°$		$\beta = 90°$	
	$\bar{P}_{solar}$	$\bar{P}_{IR}$	$\bar{P}_{solar}$	$\bar{P}_{IR}$
X+(nadir)	49.7	361.3	2.2	27.0
X-	432.0	0.0	1.8	0.0
Y+	9.0	120.3	1361.0	29.7
Y-	9.0	120.3	0.0	1.1
Z+(ram)	292.4	120.1	2.0	10.2
Z-	295.4	120.1	2.1	10.2

Units: W/m^2

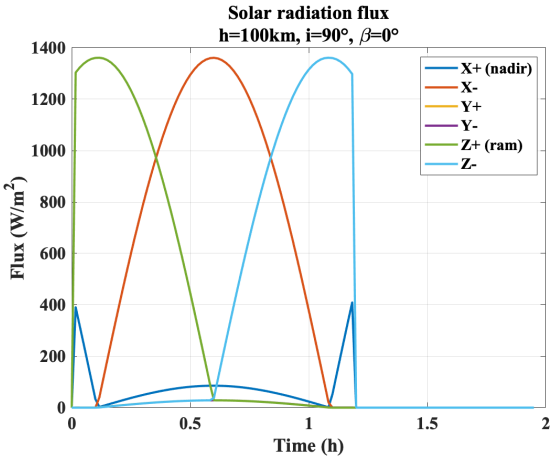

Figure 6: Solar Radiation Flux (Direct + Albedo) on Faces during Orbital Period (0° Beta-Sun angle)

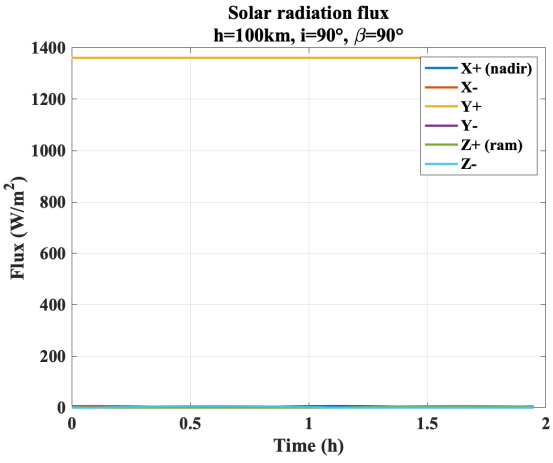

Figure 7: Solar Radiation Flux (Direct + Albedo) on Faces during Orbital Period (90° Beta-Sun angle)

Table 1 presents the orbital average values of the IR and Solar radiation fluxes received by each satellite face.

Lunar Eclipses (Earth Shadows)

Another critical aspect to consider during the thermal system design of a LLO mission is the impact of the Earth blocking the Sun. Note that a solar eclipse viewed from the Moon (the Earth being between the Sun and the Moon) would be called a lunar eclipse when viewed from Earth[4]. Figure 8 presents the duration of partial and total solar eclipses (Moon's reference) for the next decade[5].

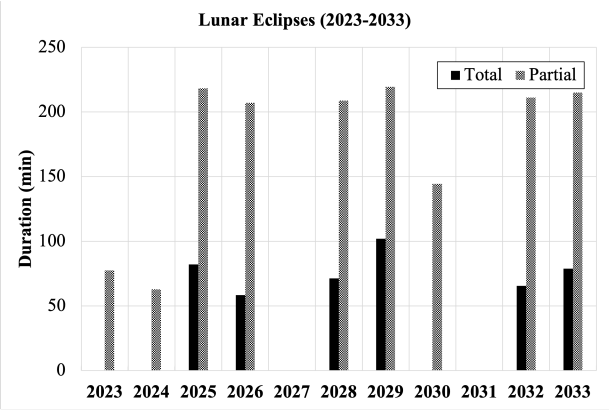

Figure 8: Partial and Total Lunar Eclipses Over the Next 10 Years

To conservatively model this condition as the worst cold case, the HLS Thermal Analysis Guidebook[4] suggests that the solar flux and albedo should be set to zero for the duration of partial and total eclipse. For example, if we consider the longest total eclipse of the next decade, happening on Jun/2029, the spacecraft should be able to survive 320 minutes (5h20) with no solar flux. In addition, since the surface temperature of the Moon's near side drops significantly during the eclipse (below 200K during the total eclipse phase), HLS Thermal Analysis Guidebook also suggested that the IR flux should be considered as low as the unilluminated side values.

Simple Thermal Model For Orbital Average Computation

Once the thermal environment of the LLO is understood, one might ask what is the maximum average internal dissipation power that a CubeSat can handle using standard passive thermal control with no deployable surfaces. To answer that question, let us consider the following simplified thermal analysis to study the effect of the optical properties of the body faces materials over the maximum orbital average internal dissipation power constrained by the maximum orbital average internal temperature of the spacecraft.

In steady-state, the spacecraft's dissipation power must equal the sum of the absorbed environmental thermal loads (Solar and Moon IR) and the internal dissipation power. For simplicity, let's assume that all six body faces share the same orbital average temperature $\bar{T}_{faces}$ and optical properties: absorptivity (α) and emissivity (ϵ). Although these assumptions are not usually accurate since the thermal resistances between faces are not negligible, and each face can be covered with different materials, they serve the purpose of a first approximation. Considering the orbital average values (indicated with a top bar on the variables), the energy balance can be expressed by Equation 4.

$$\epsilon\sigma\bar{T}_{faces}^4\sum_{i=1}^{6}A_i = \alpha\sum_{i=1}^{6}A_i\bar{P}_{solar,i} + \epsilon\sum_{i=1}^{6}A_i\bar{P}_{IR,i} + \bar{P}_0 \tag{4}$$

where

$\bar{T}_{faces}$: orbital average temperature of all faces

A_i: face i area

α: solar absorptivity of all faces

ϵ: IR emissivity of all faces

σ: Stefan-Boltzmann constant

$\bar{P}_{solar,i}$: orbital average solar flux incident on face i

$\bar{P}_{IR,i}$: orbital average IR flux incident on face i

$\bar{P}_0$: orbital average internal dissipation power

Let us consider a simple lumped parameter thermal model shown in Figure 9. A single thermal resistance connects each face node to the internal node. Since all faces are assumed to be fully thermally connected (zero thermal resistance between faces), the effective thermal resistance between the internal node and all faces, R, can be calculated by Equation 5.

$$R = (\sum_{i=1}^{6}\frac{1}{r_{0,i}})^{-1} \tag{5}$$

Where $r_{0,i}$ is thermal resistance between the internal node and the face i.

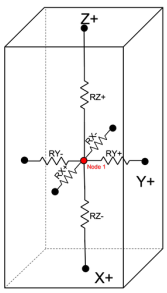

Figure 9: CubeSat - Lumped Parameter Thermal Model

Using the effective thermal resistance R, $\bar{T}_{faces}$ can be written in terms of the average internal node temperature T_0 as shown in Equation 6.

$$\begin{aligned} \bar{T}_0 - \bar{T}_{faces} &= R\bar{P}_0 \\ \bar{T}_{faces} &= \bar{T}_0 - R\bar{P}_0 \end{aligned} \tag{6}$$

Let the total body surface area be

$$A_{total} = \sum_{n=1}^{6} A_i$$

and the total environmental thermal load be

$$\bar{P}_{env}(\alpha, \epsilon) = \alpha \sum_{i=1}^{6} A_i \bar{P}_{solar,i} + \epsilon \sum_{i=1}^{6} A_i \bar{P}_{IR,i}$$

Equation 4 can be rewritten in terms of the average internal temperature $\bar{T}_0$ as shown in Equation 7.

$$\epsilon\sigma(\bar{T}_0 - R\bar{P}_0)^4 A_{total} - \bar{P}_0 - \bar{P}_{env}(\alpha, \epsilon) = 0 \tag{7}$$

Now, if the maximum average internal temperature is defined as $\bar{T}_{0,max}$, the nonlinear Equation 7 can be solved to find the maximum orbital average dissipation power $\bar{P}_{0,max}$, for a given value of R and pair of α and ϵ. To demonstrate the usage of this simple thermal mode, let us analyze the cases of 6U and 12U CubeSats in LLO.

Example 1: 6U Cubesat in Polar LLO

Consider the case of a 6U CubeSat at 100km altitude and 90° inclination with a fixed nadir-pointing orientation as shown in Figure 10.

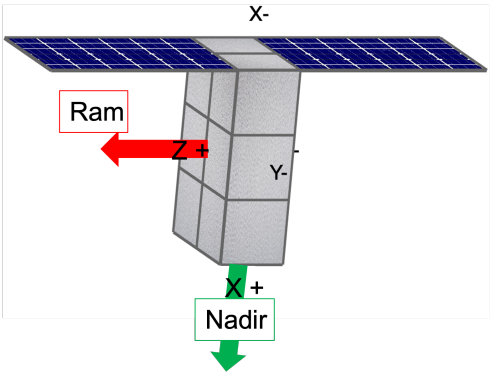

Figure 10: 6U CubeSat - Flight Configuration

To estimate the effective thermal resistance R, let us consider that the internal node is connected to each face with a thermal resistance r inversely proportional to the face size, shown by Equation 8. The value of 20K/W comes from a rough estimation using values of contact conductance found in common CubeSat stacks[6]. Since values of thermal resistances might vary significantly from this initial guess, a later analysis of the maximum internal power dissipation for different thermal resistance values is also offered.

$$r_{0,i}(\#Units) = \frac{20 \text{ K/W}}{\#Units} \tag{8}$$

If the face has a 6U size, for example, as all resistances are in parallel, then the total thermal resistance between the face node and the internal node is $r_{6U} = 20/6 \approx 3.3$K/W. Therefore, in this example of a 6U CubeSat, considering no thermal resistance between the faces' nodes, the effective thermal resistance can be calculated using Equation 5 as $R = (\frac{2}{r_{2U}} + \frac{2}{r_{3U}} + \frac{2}{r_{6U}})^{-1} \approx 0.9$K/W.

By defining the maximum orbital average internal temperature as $\bar{T}_{0,max} = 60°C$, and using the orbital average Solar and IR flux listed in Table 1, the maximum orbital average internal dissipation power, $\bar{P}_{0,max}$, can be computed solving the nonlinear Equation 7 for any combination of surface's absorptivity and emissivity coefficients. Figure 11 and Figure 12 present the results for the orbit with the Sun-Beta angle at 0° and 90°, respectively.

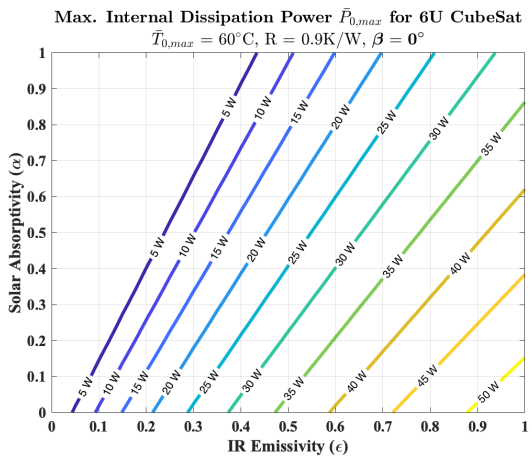

Figure 11: Avg. Dissipation Power for 60°C Avg. Internal Temperature (6U CubeSat, 0° Beta-Sun Angle)

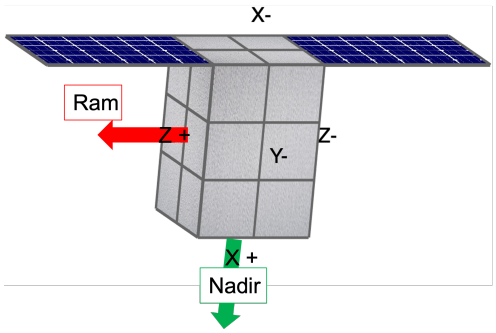

Figure 13: 12U CubeSat - Flight Configuration

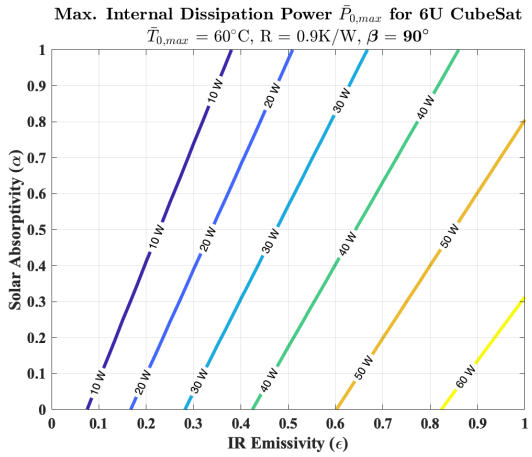

Figure 12: Avg. Dissipation Power for 60°C Avg. Internal Temperature (6U CubeSat, 90° Beta-Sun Angle)

Example 2: 12U CubeSat in Polar LLO

Similarly to the previous example, consider the case of a 12U CubeSat on lunar orbit at 100km altitude and 90° inclination with a fixed nadir-pointing orientation as shown in Figure 13.

By using the same approach from the 6U CubeSat example, the effective thermal resistance of the 12U CubeSat can be estimated as $R = (\frac{4}{r_{6U}} + \frac{2}{r_{4U}})^{-1} \approx 0.6$K/W. Figure 14 and Figure 15 present the results for the orbit with the Beta-Sun angle at 0° and 90°, respectively.

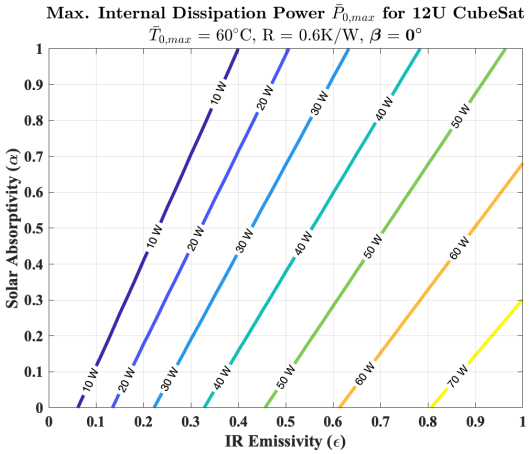

Figure 14: Avg. Dissipation Power for 60°C Avg. Internal Temperature (12U CubeSat, 0° Beta-Sun Angle)

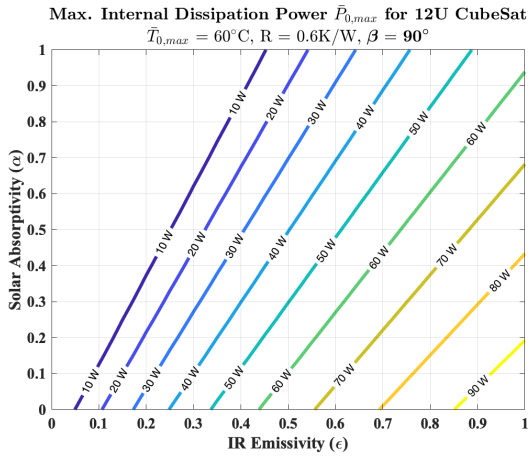

Figure 15: Avg. Dissipation Power for 60°C Avg. Internal Temperature (12U CubeSat, 90° Beta-Sun Angle)

Surface Coating Selection

The 6U and 12U CubeSat results show that the highest internal dissipation power can be achieved using coating materials with low solar absorptivity and high IR emissivity. Figure 16 shows the different thermal-optical properties values of some common spacecraft thermal control coatings grouped into seven categories[7].

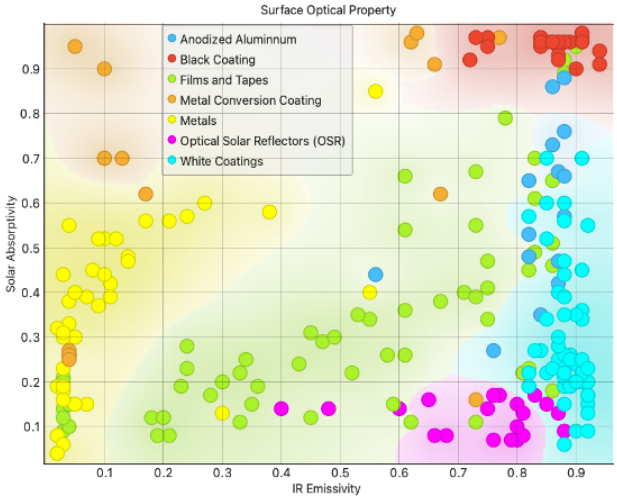

Figure 16: Absorptivity and Emissivity of Some Common Spacecraft Thermal Control Coatings

As discussed previously, the thermal resistances between the internal devices and external surfaces might differ significantly from the estimated values used in the 6U and 12U CubeSats examples. To assess the impact of different effective thermal resistance on the maximum internal power dissipation, let us assume a white coating material, like the AZ-93[8], in which absorptivity and emissivity values are 0.15 and 0.9, respectively, and solve Equation 7 for different values of R. Figure 17 presents the results. The circle markers in the plot indicate the previously estimated R values for the 6U and 12U cases.

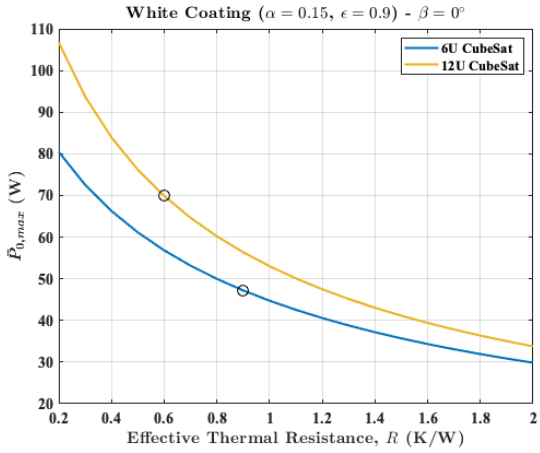

Figure 17: $\bar{P}_{0,max}$ as Function of R, Considering the AZ-93 White Coating Material Properties, $\bar{T}_0 = 60°C$

As pointed out in the Lunar Eclipse section, the thermal design must also make sure that the satellite can survive the eclipse periods encountered during its lifetime. It is important to note that while a high IR emissivity coating maximizes the internal dissipation power capacity during normal thermal environment operations, it increases the heat loss during eclipses conditions, where there is no solar flux and negligible IR flux. For high IR emissivity, the heat loss during the eclipse needs to be partially compensated by heaters to ensure that temperatures stay over the minimum allowed for each subsystem.

For long eclipses like the one in Jun/2029, the heaters' operation can deplete the CubeSat battery over its design limit. To assess this condition, let us consider that the CubeSat starts the Jun/2029 eclipse with an average internal temperature of 30°C and must end the eclipse period over -20°C. Based on an STK simulation, the spacecraft in a polar orbit at 100km altitude and 90° Beta-Sun Angle will stay under low lighting conditions for about 4 hours. Figure 18 presents the total battery energy required to keep the satellite temperature over -20°C. During the eclipse simulation, the total thermal environmental load was set to zero ($\bar{P}_{env} = 0$) to account for the colder surface temperature of the Moon.

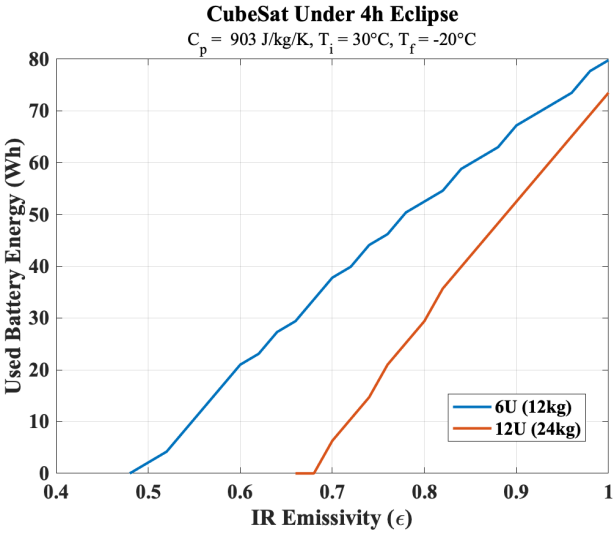

Figure 18: Battery Energy Required under Eclipse as Function of Emissivity

Although the 6U CubeSat has a smaller surface area than the 12U CubeSat, its lower thermal mass makes it lose temperature faster than the 12U, requiring more heater power. If we consider the AZ-93 white coating material emissivity of 0.9, the 6U CubeSat will draw 67Wh from the battery during the 4 hours of eclipse versus 53Wh for the 12U CubeSat. For a typical battery capacity of 87Wh for a 6U CubeSat, that long eclipse will require 77% depth of discharge.

LUNAR RADIATION ENVIRONMENT

The Moon radiation environment also poses higher risks to CubeSats when compared to a typical LEO environment. Although CubeSats in LEO are subjected to trapped radiation, especially over the South Atlantic Anomaly, the Earth's magnetosphere reduces the energy and flux of outcoming radiation: solar protons and galactic cosmic rays (CGR). A spacecraft in a lunar orbit does not have that protection, so solar proton and CGR impact the spacecraft with significantly more energy. Using the SPENVIS tool[9], the Total Ionization Dose (TID) over silicon-based materials for a 1-year mission in LLO can be compared against two familiar Earth orbits for CubeSats: Sun-synchronous (SSO) and ISS orbits.

Table 2 presents the SPENVIS inputs for both Earth orbits. For the LLO case, the orbit type utilized in the tool was near Earth interplanetary, with no trapped radiation and the same solar particle models and settings used for the ISS and SSO cases, with the exception that no magnetic shielding is considered. Since the tool does not take into account the Moon shielding during unilluminated phases of the lunar orbit, the TID dose was corrected for the 1-year average sun exposure time of 73%, computed for the 100km altitude and 90° inclination orbit. For reference, the sun exposure time is 65% and 61% for 60° and 30° orbital inclination, respectively, at the same altitude.

Table 2: Spenvis Inputs for ISS and SSO orbits

Coordinate Generators		
Type	ISS General/ Circular	SSO Helio-synchronous
Altitude (km)	500	500
Inclin. (deg)	51.6	98
Representative (days)	30	30
Radiation sources and effects		
Trap. Radiation Model	AP-8/AE-8	
Model Version	Solar Maximum	
Solar particle model (1-yr Mission)	ESP-PSYCHIC (total fluence)	
Solar particle model (SPE)	ESP-PSYCHIC (worst event fluence)	
Confidence level	95%	
Mag. shielding	On (Quiet magnetosphere)	
Dose model	SHIELDOSE-2	
Shild. Configuration	Centre of Al sphere	
Target material	Silicon	

Figure 19 contrasts the TID experienced by the spacecraft in a 1-year mission in LLO in opposition to missions in typical low Earth orbits. The 2krad and 20krad thresholds, shown in the plot, indicate the dose levels at which typically commercial and semihard parts begin to encounter effects, respectively[10]. However, it is important to note that each component's radiation tolerance might vary significantly from those values. A TID test conducted at the University of Massachusetts Lowell Radiation Laboratory using a high-dose rate Cobalt-60 gamma source showed that even some commercial microcontrollers and SD cards, commonly used in CubeSats, can resist up to 24krad without noticeable degradation[11]. Testing critical COTS components using the Cobalt-60 method covered by method 1019.7 in MIL-STD883G can be an inexpensive option to avoid the need for rad-hard components[12].

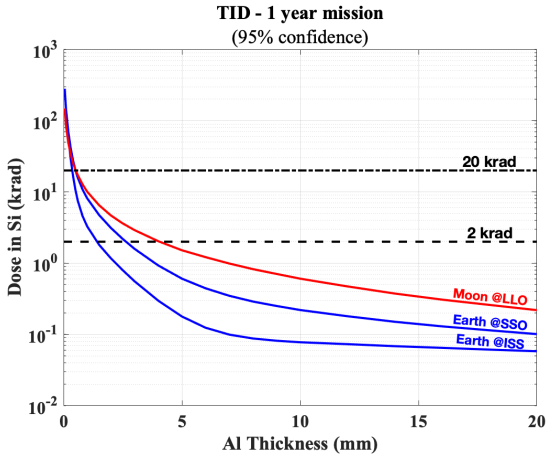

Figure 19: TID for 1-Year Mission during Solar Maximum

Solar Particle Events

Without the Earth's magnetic shielding, a Solar Particle Event can rapidly increase the radiation dose received by the spacecraft in LLO. Due to the unpredictability of SPE occurrence, magnitude, duration, and spectral characteristics, a statistical approach must be taken to find the necessary level of protection based on the mission's risk tolerance. The Emission of Solar Proton (ESP) model allows the expected worst case event fluence to be calculated for a given confidence level and mission time. This model is based on a statistical analysis of the SPE data collected during three solar cycles (20-22)[13]. Using the ESP model for the worst event case and SHIELDOSE-2 in SPENVIS, the TID from SPE occurrences was computed using a 95% confidence level for a 1-year mission period. Figure 20 presents the results for the LLO and the typical LEOs for comparison.

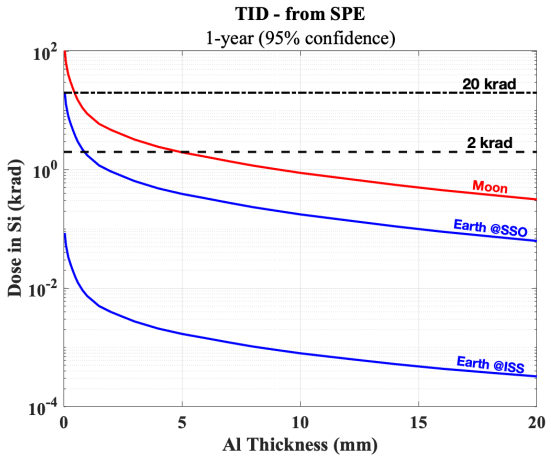

Figure 20: TID on Silicon from SPE

Considering an active solar year, assuming 5mm aluminum shielding, the total TID, considering SPE, can be estimated by the sum of the values found in Figures 19 20 as equal to 3.5 krad with 95% confidence. The TID can only be expected to be under the 2 krad threshold for a shielding thickness higher than 8mm. Figure 21 presents the estimated mass for the CubeSat chassis if considering a whole-body radiation shielding approach. For 8mm thickness walls, the estimated chassis masses are 4.3 kg and 6.4 kg for 6U and 12U CubeSats, respectively. Assuming 2 kg per CubeSat unit of total mass, those chassis masses would be about 35% and 27% of the total CubeSat masses. A probably better approach to reduce the impact of the shielding on the CubeSat mass is to shield on the components level, taking into consideration their different radiation tolerance levels.

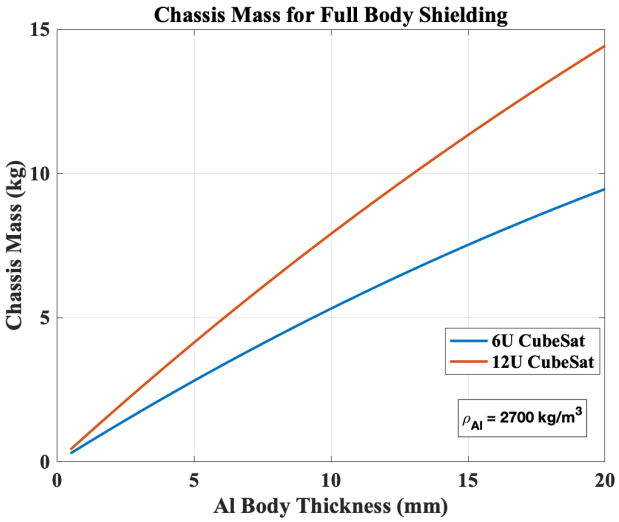

Figure 21: CubeSat Chassis Mass for Full-Body Al Shielding

CONCLUSION

The lunar thermal environment presents numerous challenges for a CubeSat thermal design. For a polar LLO, when the spacecraft orbit passes over the subsolar region (low Sun-Beta angles), the orbital average IR flux on the nadir face can reach up to $360 W/m^2$, which is 50% higher than in LEO. On the other hand, when the orbit is over the terminator region (high Beta-Sun angle), the orbital average IR flux gets as low as $27 W/m^2$. For a 100km altitude polar orbit, that orbital transition occurs every three months, which is the time for a 90° Beta-Sun angle drift. In addition, the spacecraft stays for about 40 consecutive days without solar flux interruptions as it flies over the terminator.

The thermal analysis using a simple thermal model shows that 6U and 12 CubeSats can dissipate the most power, assuming only passive thermal control and no deployable

surfaces, by having surface properties with low solar absorptivity and high IR emissivity. Considering a maximum average internal temperature of 60°C, 6U and 12U CubeSats can potentially dissipate up to 50W and 70W of average orbital power, respectively. That assumes that their surfaces are finished with a white coating material. The effective thermal resistance between the internal node and the external surfaces is 0.9K/W for the 6U and 0.6K/W for the 12U CubeSat. It was also shown that the maximum dissipation power could be maximized by reducing the effective thermal resistance, which can be achieved by improving the contact of the heat-dissipating devices with the chassis walls.

A clear disadvantage of a high IR emissivity appears in the event of a long solar eclipse (lunar eclipse if seen from Earth). During the eclipse, the solar flux drops to zero, and the planetary IR flux decreases significantly due to the rapid cooling of the Moon's surface. The simulation showed that to keep the internal temperature over -20°C during a 4 hours eclipse, like the one expected in Jun/2029, whited-coated 6U and 12U CubeSats would require at least 67Wh and 53Wh of heating energy, respectively, assuming the same previous values of internal thermal resistances. That amount of energy must be available in the battery before the beginning of the eclipse, which requires proper battery sizing, performance, and operational planning.

The lunar radiation environment can be significantly more dangerous for CubeSats than typical low Earth orbits such as the ISS orbit and SSO. Without considering extreme solar events, the TID on silicon for a 1-year mission in LLO was computed to be 2.5 times higher than for the SSO and about 9 times higher than for the ISS orbit. If SPEs are considered with 95% confidence during the 1-year mission, the TID from SPE in LLO is about 5 times higher than for the SSO. By aggregating the TID from regular proton fluence and SPE, the simulation shows that at least 8mm of aluminum shielding would be required to keep the TID below 2krad with 95% confidence in LLO during solar maximum. For a full-body shielding approach, 8mm of wall thickness would cause the chassis mass to be around 35% and 27% of the total mass for the 6U and 12U CubeSats, respectively, assuming 2kg per unit, which suggests that the shielding should be performed at the components level for a typical mass-constrained mission, tailored by their different radiation tolerances.

REFERENCES

1. Jennifer Harbaugh. Space Launch System Orion Stage Adapter (OSA), November 2021.
2. CAPSTONE Team Stops Spacecraft Spin, Clearing Hurdle to Recovery – Artemis, October 2022.
3. Romain Peyrou-Lauga. Using Real Earth Albedo and Earth IR Flux for Spacecraft Thermal Analysis. July 2017. Accepted: 2017-07-07T16:16:19Z Publisher: 47th International Conference on Environmental Systems.
4. *Human Landing System Lunar Thermal Analysis Guidebook*, volume HLS-UG-001. NASA, 2021.
5. Catalog of Lunar Eclipses: 2001 to 2100.
6. Philipp Hager, Tobias Flecht, Katja Janzer, Laura Leon Perez, Hugo Brouwer, and Martin Jonsson. Contact Conductance in Common CubeSat Stacks. July 2019. Accepted: 2019-06-21T19:44:57Z Publisher: 49th International Conference on Environmental Systems.
7. J. H. Henninger. Solar absorptance and thermal emittance of some common spacecraft thermal-control coatings. Technical report, April 1984. NTRS Author Affiliations: NASA Goddard Space Flight Center NTRS Report/Patent Number: REPT-84F0248 NTRS Document ID: 19840015630 NTRS Research Center: Legacy CDMS (CDMS).
8. AZ-93 White Thermal Control, Inorganic Paint / Coating.
9. SPENVIS - Space Environment, Effects, and Education System.
10. Vincent L. Pisacane. *The Space Environment and Its Effects on Space Systems, Second Edition*. American Institute of Aeronautics and Astronautics, Inc., Reston, VA, July 2016.
11. Frank Hall Schmidt, Kerri Cahoy, Devon A. Sklair, William J. Blackwell, I. Osarentin, Robert S. Legge Jr, and Ryan W. Kingsbury. TID Tolerance of Popular CubeSat Components. In *MIT web domain*, July 2013. Accepted: 2013-09-25T19:21:31Z.
12. Doug Sinclair and Jonathan Dyer. Radiation Effects and COTS Parts in SmallSats. *Small Satellite Conference*, August 2013.
13. M.A. Xapsos, G.P. Summers, J.L. Barth, E.G. Stassinopoulos, and E.A. Burke. Probability model for worst case solar proton event fluences. *IEEE Transactions on Nuclear Science*, 46(6):1481–1485, December 1999. Conference Name: IEEE Transactions on Nuclear Science.